Look for efficient Pr–Ni based SOCs oxygen electrodes in the Ruddlesden - Popper series: preliminary thermal stability studies focused on PrNiO3-δ and (Pr, La)4Ni3O10+δ

Vaibhav Vibhu, Romuald Frugier, Rüdiger-A. Eichel, Jacinthe Gamon, Jean-Marc Bassat

Look for efficient Pr-Ni based SOCs oxygen electrodes in the Ruddlesden - Popper series: preliminary thermal stability studies focused on $PrNiO_{3-\delta}$ and $(Pr, La)_4Ni_3O_{10+\delta}$

Vaibhav Vibhu[1, 2, #], Romuald Frugier[1, #], Rüdiger-A. Eichel[2], Jacinthe Gamon[1] and Jean-Marc Bassat[1,*]

[1] *CNRS, Université de Bordeaux, Institut de Chimie de la Matière Condensée de Bordeaux (ICMCB), 87 Av. Dr Schweitzer, F-33608 Pessac Cedex, France.*

[2] *Institute of Energy Technologies, Fundamental Electrochemistry (IET-1), F, Forschungszentrum Jülich GmbH, 52425 Jülich, Germany*

* *Corresponding author: jean-marc.bassat@icmcb.cnrs.fr*

[#] *These authors contributed equally to the publication as first authors*

Abstract

The present work investigates the thermal stability of Pr-Ni based nickelates belonging to the Ruddlesden-Popper (RP) series, namely: $Pr_4Ni_3O_{10+\delta}$, $La_4Ni_3O_{10+\delta}$, $La_3PrNi_3O_{10+\delta}$ (n=3), and $PrNiO_{3-\delta}$ (n = ∞). Indeed these nickelates can be used as future oxygen electrodes in Solid Oxide Cells devices operating at high temperature, and a preliminary work is mandatory to get accurate information about the required conditions (mainly temperature and pO_2) to successfully synthesize, sinter and use those materials as electrodes. Three different atmospheres, *i.e.* argon, air and oxygen were here considered. As expected the thermal stability is higher under pure oxygen compared to air, and higher under air compared to argon. Depending on the material a complete and irreversible decomposition can be observed. Finally, accurate results were obtained according to our dynamic study, which is based on TGA and XRD experiments.

Keywords: Solid oxide cells (SOCs), Nickelates, Chemical stability, Thermal stability

1. Introduction

Because most of the renewable energy sources for electricity production work intermittently, perspectives to be considered must be related to chemical storage of excess electricity. In that matter, power to gas or fuel technologies, using water (possibly combined to CO_2) electrolysis appear as attractive solutions. For this purpose, the stationary devices often use high temperature electrolysers because of their high efficiency. The corresponding technology involves Solid Oxide Cells (SOCs), possibly combining electrolysis (Solid Oxide Electrolysis Cells, SOECs) and fuel cells (Solid Oxide Fuel Cells, SOFCs) in a reversible mode (H_2 production and conversion, respectively) [1]. The continuous research to improve the high temperature SOC electrochemistry converged in studies focused on lanthanide nickelates over the past 20 years [2], emphasizing their excellent performances as oxygen electrodes for IT-SOC devices operating at intermediate temperatures (600-700°C). These materials belonging to the Ruddlesden-Popper (RP) series *i.e.* $Ln_{n+1}Ni_nO_{3n+1}$ (n = 1, 2, 3) are considered as the second generation of oxygen electrodes for devices operating either under SOFC or SOEC modes [3-5]. In this respect, RP nickelates with n=1, *i.e.* $Ln_2NiO_{4+\delta}$ (Ln = La, Pr, Nd) have been extensively studied [6-11]. These compounds with the K_2NiF_4 -type layered structure show promising cathode performance for IT-SOFCs because of their large anionic bulk diffusion and surface exchange coefficients, combined with good electrical conductivity and thermal expansion properties matching with those of other components of the cell [12-14]. Among the $Ln_2NiO_{4+\delta}$ (Ln = La, Pr, Nd), $Pr_2NiO_{4+\delta}$ appears to be the most efficient SOFC oxygen electrode [7, 15], exhibiting excellent electrochemical properties at intermediate temperature, for instance R_p = 0.15 Ω·cm² at 600 °C measured on screen printed electrodes

($Pr_2NiO_{4+\delta}$//CGO//8YSZ symmetrical half-cell) [16]. However, this material is thermally unstable and decomposes rapidly into $Pr_4Ni_3O_{10+\delta}$, $PrNiO_{3-\delta}$, Pr_6O_{11} and NiO [17-19].

The three Pr-based materials issued from the decomposition mentioned above have already been studied as electrodes with very interesting properties, in particular, Pr_6O_{11} and $Pr_4Ni_3O_{10+\delta}$ have shown excellent single cell performance under SOFC conditions. For example, the single cell where the oxygen electrode is Pr_6O_{11} infiltrated into a porous GDC backbone, *i.e.* NiO-YSZ//YSZ//GDC-Pr_6O_{11}, shows a maximum power density of 0.83 $W \cdot cm^{-2}$ at 600 °C [20].

The $Pr_4Ni_3O_{10+\delta}$ phase also shows promising electrochemical performance with similar R_p value as that of $Pr_2NiO_{4+\delta}$ (0.15 $\Omega \cdot cm^2$ at 600 °C for the symmetrical half-cell). In addition, the single cell with $Pr_4Ni_3O_{10+\delta}$ oxygen electrode and GDC barrier layer prepared by screen-printing, *i.e.* NiO-YSZ//YSZ//GDC//$Pr_4Ni_3O_{10+\delta}$ shows a maximum power density of 1.6 and 0.68 $W \cdot cm^{-2}$ at 800 and 700 °C, respectively [21]. Furthermore, the single cell containing $Pr_4Ni_3O_{10+\delta}$ as oxygen electrode showed stable behaviour during long-term operation under SOFC conditions at a constant current load of 0.3 $A \cdot cm^{-2}$ at 700 °C and a degradation rate of less than 1%/kh was observed [22].

Finally, despite very good chemical stability and electronic conductivity, $PrNiO_{3-\delta}$ shows the highest R_p values among the series [23]. For instance, the symmetrical half-cell with $PrNiO_{3-\delta}$ electrode prepared by screen-printing over a GDC barrier layer ($PrNiO_{3-\delta}$//CGO//8YSZ symmetrical half-cell co-sintered together at 950 °C/2h) shows an R_p value of 0.91, 0.12 and 0.03 $\Omega \cdot cm^2$ at 600, 700 and 800 °C respectively, however without optimization of the sintering conditions [24]. Therefore, optimizing the sintering conditions can further improve the electrochemical performance of $PrNiO_{3-\delta}$. Prior to further optimisation of the sintering process, however, determining the phase

stability conditions with temperature and under different atmospheres is essential and has to be investigated.

With regards to the stability of $Pr_4Ni_3O_{10+\delta}$, studies were already carried out and it was concluded that the thermal stability limit is around 1050°C in air, and around 1120°C in oxygen [21]. However, the stability of $Pr_4Ni_3O_{10+\delta}$ in an argon atmosphere is still unknown in the literature to the best of our knowledge. Moreover, to further improve the thermal stability of $Pr_4Ni_3O_{10+\delta}$ phases, we have prepared the $(Pr, La)_4Ni_3O_{10+\delta}$ solid solution and investigated its thermal stability as a function of temperature and pO_2.

In this work, with the aim to comprehensively investigate the suitability of Pr- and Ni-based oxides (n = 3 and n = ∞ (perovskite-type) terms of the RP series) as oxygen electrodes, the thermal stabilities in argon, air and oxygen atmospheres are compared, allowing further determination of the most suitable sintering and operating conditions. Themogravimetry (TGA) experiments in combination with X-ray diffraction (XRD) were mainly used for the investigations. Moreover, both air, oxygen and also argon atmospheres were considered. Indeed in the case of metal-supported cells it becomes mandatory to perform the first part of the sintering procedure under reducing atmosphere (to avoid any detrimental oxidation of the metal support, and prior to the re-oxidation of the oxygen electrode which is performed in a second step on the tight complete cell).

2. Experimental

2.1. Synthesis of powders

$PrNiO_{3-\delta}$ was synthesized using the citrate-nitrate route (modified Pechini method) from Pr_6O_{11} (Aldrich Chem, 99.9%), and $Ni(NO_3)_2.6H_2O$ (Acros Organics,

99%) precursors [25]. The Pr_6O_{11} powder was pre-fired at 900 °C overnight to remove the remaining water content due to its highly hygroscopic character. After the auto combustion step, a final annealing was performed at 850 °C for 48 h under oxygen flow and repeated eight times leading to well crystallized phases.

The $(Pr, La)_4Ni_3O_{10+\delta}$ phases were also synthetized using the citrate-nitrate route from a commercial $Pr(NO_3)_3$ solution (Rhodia), $La(NO_3)_3.6H_2O$ (Thermo-scientific, 99.9%) and $Ni(NO_3)_2.6H_2O$ (Thermo-scientific, 99%) precursors. The xH_2O content of the precursors was determined by a pre-firing step. After pyrolysis, a pre-calcination step was carried out before the final annealing performed at 1050°C under air for $La_4Ni_3O_{10\pm\delta}$/ $La_3PrNi_3O_{10\pm\delta}$ or pure oxygen for $Pr_4Ni_3O_{10\pm\delta}$ [26].

The ageing test of the four studied phases was performed under air. Pellets were first prepared and then left into a furnace for one then three months at 600, 700 and 800 °C before XRD characterization.

2.2. X-ray diffraction analysis

The powders were first investigated by X-Ray diffraction (XRD) at room temperature using a PANanalytical X'pert MPD diffractometer with Cu-K_α incident radiation to check the phase purity. The X-ray diffraction patterns were fitted by profile matching using the Fullprof software [27].

2.3. Thermal gravimetric analyses (TGA)

TGA experiments were carried out using a TA Instrument® TGA-5500 and Q600 device. In a first step, the studied material was heated in air up to 800 °C then cooled down to room temperature with a slow rate (2 °C.min^{-1}), this cycle being reproduced twice to ensure the reproducibility and an efficient equilibration of the material with the

surrounding atmosphere. In a second step, the determination of the oxygen stoichiometry was achieved *via* the full decomposition of the material into Ni metal and Pr_2O_3 under Ar -5% H_2 flux with a very slow heating rate (0.5 °C.min^{-1}). Moreover, in order to *i)* to investigate its thermal stability in the various atmospheres and *ii)* to study the δ variation *vs. T* in the domain of stability, TGA measurements were performed up to T_{max} = 1200°C, under air (pO_2 = 0.21 atm), oxygen (pO_2 = 1 atm) and argon atmosphere ($pO_2 \approx 10^{-5}$ atm). Different heating and cooling rates were used as detailed below.

In addition, we chose to study the effect of kinetics on the decomposition of $PrNiO_{3-\delta}$, which is the most oxidized and less stable phase at high temperature. For this, several thermal cycling were performed with the heating and cooling rate of 2 °C.min^{-1} for a different dwell time 1h, 2h, 3h and 5h at 1000 °C and 950°C. The variations of weight during heating and cooling were investigated.

3. Results and discussion

3.1. XRD Analysis recorded on the as-prepared powders

The XRD characterizations of all nickelates *i.e.* $PrNiO_{3-\delta}$ and $(Pr, La)_4Ni_3O_{10+\delta}$ reveal that all phases are well crystallized. The crystallographic parameters of the as-prepared powders are gathered in table 1 and the corresponding XRD diagrams are plotted in Fig. S.I. 1. The phase $PrNiO_{3-\delta}$ was described by an orthorhombic structure with *Pbnm* space group [24]. The crystal structure of n=3 RP phases is still under debate in the literature. Through neutron diffraction study, it was revealed that $La_4Ni_3O_{10}$ and $La_3PrNi_3O_{10}$ crystallizes in the orthorhombic space group *Bmab* [28, 29], while $Pr_4Ni_3O_{10}$ was best fitted using the $P2_1/a$ monoclinic space group [30].

Material	n-value	a (Å)	b (Å)	c (Å)	β (°)
$Pr_4Ni_3O_{10\pm\delta}$	3	5.37803 (8)	5.4631 (1)	27.5644 (7)	90.283 (2)
$La_3PrNi_3O_{10\pm\delta}$		5.4039 (1)	5.4648 (1)	27.897 (2)	89.811 (4)
$La_4Ni_3O_{10\pm\delta}$		5.4165 (1)	5.4652 (1)	27.971 (1)	90.173 (6)
$PrNiO_{3-\delta}$	∞	5.4254 (4)	5.3882 (5)	7.6414 (4)	90

Table 1- Cells parameters determined on the as-prepared powders

3.2. Thermal stability studies performed on $PrNiO_{3-\delta}$

3.2.1. Thermal stability under argon, air and oxygen

The initial (room temperature) δ value was firstly determined by TGA measurement performed under Ar/5%H_2 atmosphere (heating/cooling rate: 2°C.min^{-1}) on the air-prepared material δ: = 0.055. The thermal stability under argon, air and oxygen atmospheres was then investigated in order to find the most appropriate sintering conditions as SOC oxygen electrodes. The comparison of the weight loss variation with temperature shows very different behaviours depending on the atmosphere (Fig. 1). Under argon, $PrNiO_{3-\delta}$ is only stable up to ~ 800 °C. Above this temperature, the material directly changes into $Pr_2NiO_{4+\delta}$ and NiO, the dissociation being complete at 1000 °C as confirmed by XRD analysis at the end of cooling (Fig. 2a). Any further significant evolution is observed during cooling.

Under air and oxygen atmosphere, $PrNiO_{3-\delta}$ exhibits a more extended stability range than under argon, as expected. The phase is stable up to 1000 °C under air, and then starts decomposing into $Pr_4Ni_3O_{10+\delta}$ and NiO. This is attested by a side experiment where an XRD analysis of the powder after quenching performed from 1050°C under air (Fig.S.I. 2). However, the $Pr_4Ni_3O_{10+\delta}$ phase remains stable only over a very short temperature window (~ 1045−1055 °C) (small deceleration on Fig. 1 for this temperature range).

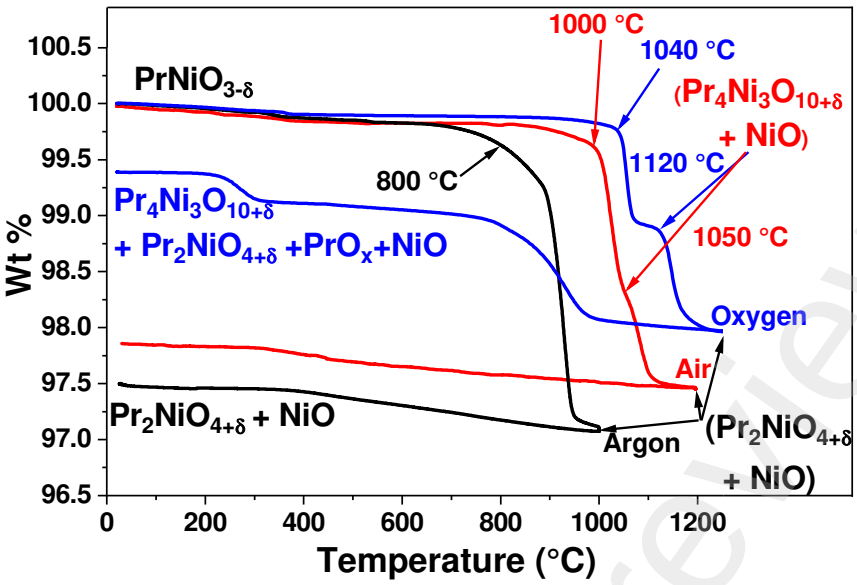

Fig. 1: Variation of the weight loss with temperature for $PrNiO_{3-\delta}$ recorded under argon, air and oxygen atmospheres with 2°C.min^{-1} heating and cooling rates

Above 1050°C, $Pr_2NiO_{4+\delta}$ and NiO are again formed and remain upon cooling. Finally, this behaviour after the thermal cycle performed under air is close to what is observed under argon (Fig. 2a).

Among the three atmospheres, $PrNiO_{3-\delta}$ shows maximum stability, up to 1040 °C, under oxygen (Fig. 1). Above this temperature, similarly to what was observed under air, it decomposes into $Pr_4Ni_3O_{10+\delta}$ and NiO (as attested by a side experiment where an XRD analysis of the powder was performed after quenching the powder from 1070°C under oxygen, Fig. S.I. 2.). Again the $Pr_4Ni_3O_{10+\delta}$ phase is only stable in a short temperature window (~ 1050–1120 °C). Above ~ 1120 °C $Pr_2NiO_{4+\delta}$ and NiO are only present (Fig. 1.). Very interestingly, the cooling behaviour under oxygen is completely different from that previously observed under air or argon. With a cooling rate of 2 °C.min^{-1}, $Pr_2NiO_{4+\delta}$ again starts changing into $Pr_4Ni_3O_{10+\delta}$ and PrO_x (around 950°C). With respect to the XRD analysis of Fig. 2c (at the end of the cooling process performed under oxygen), it is evidenced that the remaining amount of $Pr_2NiO_{4+\delta}$ is very limited,

and one can imagine that a longer plateau at T = 1200°C would allow to achieve a complete decomposition of $Pr_2NiO_{4+\delta}$.

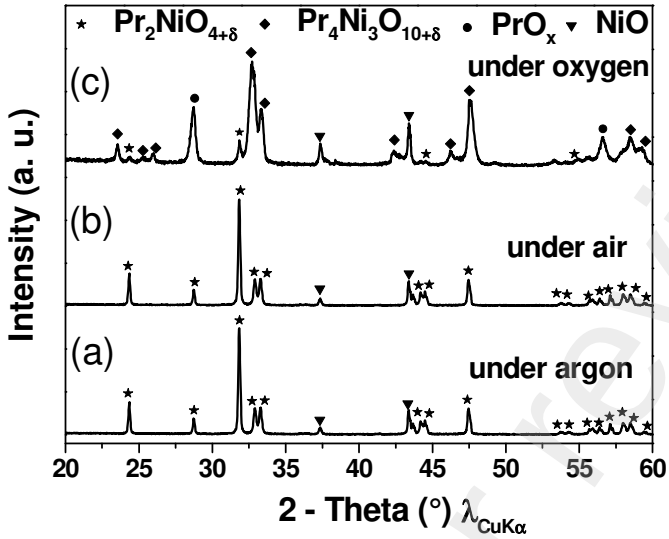

Fig. 2: X-ray diffractograms of the $PrNiO_{3-\delta}$ powders after TGA under (a) argon, (b) air and (c) oxygen

In addition, first aiming at better understanding the thermal behaviour under oxygen, various heating and cooling rates, namely 1°, 2° and 5 °C.min^{-1} up to 1300 °C were used. The TGAs curves recorded at the different rates are plotted in Fig. S.I. 3a, b, and c. Higher heating and cooling rates (5 °C.min^{-1}) prevent the formation of $Pr_4Ni_3O_{10+\delta}$ leading to a final mixture of $Pr_2NiO_{4+\delta}$, PrO_x and NiO as end products.

Finally, the derivatives corresponding to the thermal evolutions of $PrNiO_{3-\delta}$ observed during heating and cooling (performed at different rates), under argon, air and oxygen atmospheres are gathered in Fig. S.I. 4.

To summarize, one can conclude that the maximum temperature at which $PrNiO_{3-\delta}$ is stable varies from 800 °C to 1000 °C and 1040 °C under argon, air and oxygen, respectively. When heated above these temperatures, the decomposition into

$Pr_2NiO_{4+\delta}$ and NiO seems to be irreversible under argon and air. Under an oxygen cycle including a cooling step performed with low rate, $Pr_2NiO_{4+\delta}$ is mostly changed into $Pr_4Ni_3O_{10+\delta}$.

3.2.2. Variation of oxygen content under argon, air and oxygen

Remaining in the stability domain of $PrNiO_{3-\delta}$ in the different considered atmospheres (see above), the variation of the oxygen content was studied by TGA. For each atmosphere, two cycles were performed to check the reversibility while the powder was kept for 1 hour at the maximum temperature before cooling. In all atmospheres, a reversible behaviour is observed (Fig. 3), the second cycle being only plotted here. A drop in $3-\delta$ is observed whatever the considered atmosphere. It occurs at lower temperature under Ar ($T \approx 680$ °C) in relation with a slightly larger drop of about 0.04, while under air and oxygen, a smoother drop of about 0.025 is observed for T above 700 °C. However, those absolute values have to be considered with care as, for instance, the equilibrium time of 1h appears not sufficient under Ar atmosphere (*i.e.* a small difference is observed between cooling and further heating).

After the different thermal cycles (Fig 3), the room-temperature δ value in $PrNiO_{3-\delta}$ decreases from 0.06, 0.055 and 0.05 when the materials were annealed under argon, air and oxygen, respectively. In other words, the content of oxygen is maximum (~ 2.95) under oxygen and slightly decreases in air (~ 2.945) and a bit more in argon (2.94).

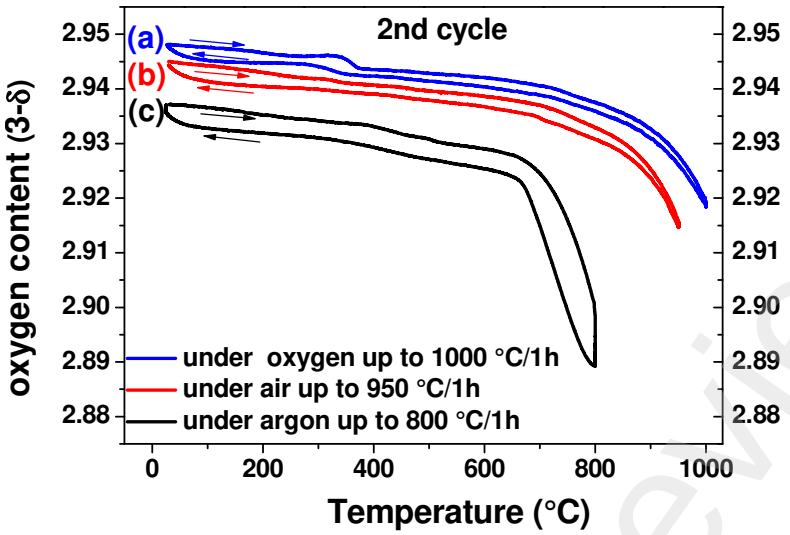

Fig. 3: Thermal variation of the oxygen content (3-δ) of $PrNiO_{3-\delta}$, (a) under oxygen (30 °C ≤ T ≤ 1000 °C), (b) under air (30 °C ≤ T ≤ 950 °C) and (c) under argon (30 °C ≤ T ≤ 800 °C).

3.2.3. Stability above 950 °C and in operating SOFCs condition

To go further in the investigation of the stability duration at 1000 °C and 950 °C under oxygen and air respectively (as a maximum stability temperature under these atmospheres), additional TGA experiments were carried out. In the frame of this work, Argon was no more considered because the upper limit of thermal stability is too low with respect to the usual conditions of preparation of the electrodes (950 °C/1h). For this purpose several cycles were performed in each case with the heating and cooling rate of 2 °C.min^{-1} for different dwell times: 1, 2 and 3 h at 1000°C under oxygen and up to 5 hours at 950°C under air. The variations of weight during heating and cooling are plotted in Fig. 4 (a, b).

Under oxygen, the $PrNiO_{3-\delta}$ phase is stable during the first two cycles and shows almost reversible behaviour. However, in the third cycle, then for a total dwelling time of 3 h, a large weight loss associated with a partial decomposition of $PrNiO_{3-\delta}$ into $Pr_4Ni_3O_{10+\delta}$ + PrOx + NiO is observed, as confirmed by XRD (Fig. S.I. 5).

Under air, $PrNiO_{3-\delta}$ phase is only stable up to 4 h at 950 °C, for longer time it also starts decomposing into $Pr_4Ni_3O_{10+\delta}$, PrOx and NiO, as confirmed by XRD (Fig. S.I. 5). Similarly, Martinez-Lope *et al.* reported the thermal stability of $PrNiO_{3-\delta}$ under air up to 900 °C up to 4 hours [31].

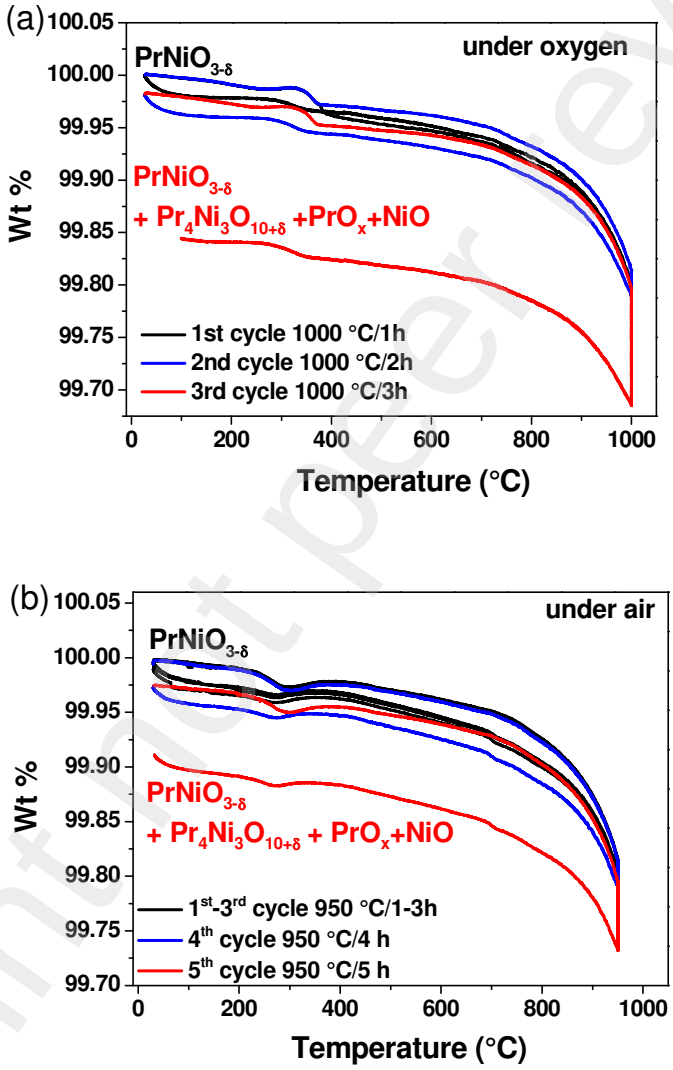

Fig. 4: Thermal variation of the oxygen content (3-δ) of $PrNiO_{3-\delta}$, (a) under oxygen (30 °C ≤ T ≤ 1000 °C) for various dwell times 1h, 2h and 3h at 1000 °C (b) under air (30 °C ≤ T ≤ 950 °C) for different dwell times 1 h, 2 h, 3 h, 4h and 5 h at 950 °C (with heating and cooling rate of 2 °C.min^{-1}).

3.2.4. Long term chemical stability of $PrNiO_{3-\delta}$ powder under air at operating conditions

The XRD patterns of $PrNiO_{3-\delta}$ powder after ageing for one month at 600, 700 and 800 °C under air along with as prepared powder are compared in Fig. 5. Overall, there is no modification of the XRD pattern after the ageing period. The $PrNiO_{3-\delta}$ powder is chemically stable at the operating temperature of SOFCs *i.e.* 600, 700 and 800 °C under air up to 1 month.

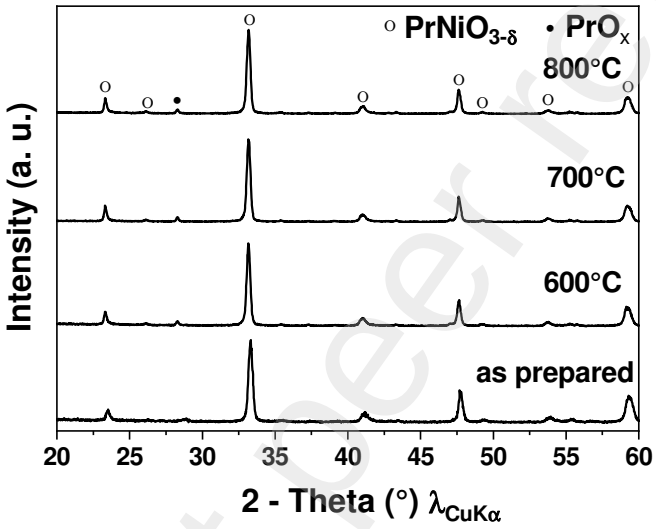

Fig. 5: X-ray diffractograms of $PrNiO_{3-\delta}$ as prepared and after ageing for 1 month at 600, 700 and 800 °C, under air.

3.3 Thermal stability studies performed on $(Pr, La)_4Ni_3O_{10+\delta}$

Our goal here was to study three compositions: $Pr_4Ni_3O_{10+\delta}$, $La_4Ni_3O_{10+\delta}$, and $La_3PrNi_3O_{10+\delta}$; indeed, with respect to our study of the corresponding n=1 series, substituting 25% of La by Pr was a very efficient way to improve both the thermal stability and at the same time the electrochemical properties of the electrode [17].

3.3.1. Thermal stability under air, O_2 and Ar

The initial (room temperature) δ values were firstly determined by TGA measurements performed under Ar/5%H_2 atmosphere on the air-prepared (Pr, La)$_4Ni_3O_{10+\delta}$ materials, the results are: δ = 0.10 for $Pr_4Ni_3O_{10+\delta}$, 0.06 for $La_4Ni_3O_{10+\delta}$ and 0.05 for $La_3PrNi_3O_{10+\delta}$.

The temperature stability limit was assessed by TGA performed under air and O_2 up to ≈ 1200 °C for $Pr_4Ni_3O_{10+\delta}$, $La_3PrNi_3O_{10+\delta}$ and $La_4Ni_3O_{10+\delta}$. The results are plotted on Figures 6a, 6b and 6c, respectively. XRD measurements were performed after the TGAs experiments, the results are gathered in Table 2. The behaviour of $Pr_4Ni_3O_{10+\delta}$ under air and oxygen was already studied in our previous paper [21]; fig 6a gathers these data which have been completed with the measurements performed under Ar.

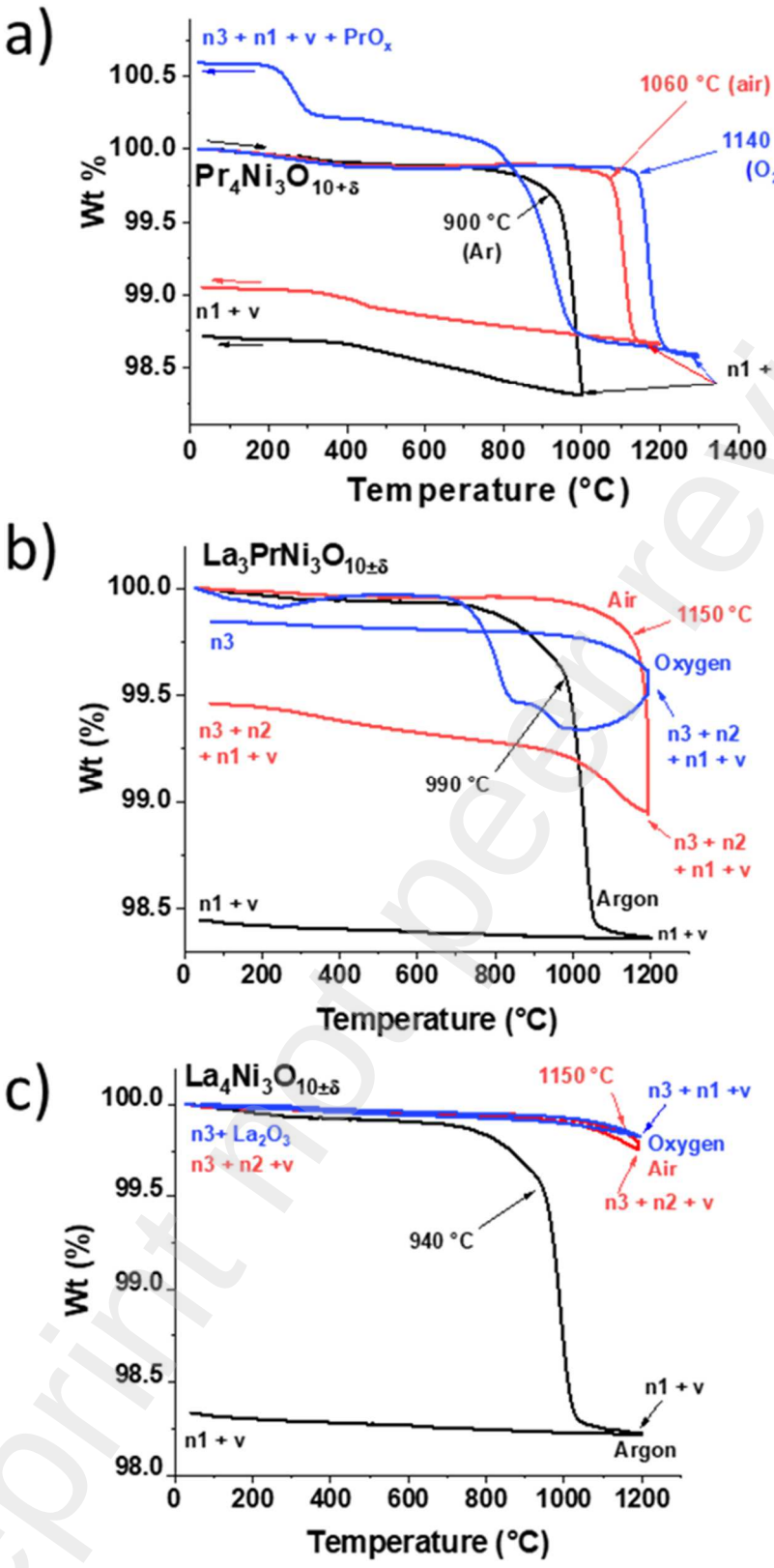

Fig.6 – TGA measurements performed under air, O_2 and Ar up to T = 1200°C on $Pr_4Ni_3O_{10+\delta}$ (a), $La_3PrNi_3O_{10+\delta}$ (b) and, $La_4Ni_3O_{10+\delta}$ (c). Where n1, n2, n3 and v correspond to $La_{2-x}Pr_xNiO_{4+\delta}$, $La_{3-x}Pr_xNi_2O_{7\pm\delta}$, $La_{4-x}Pr_xNi_3O_{10\pm\delta}$, and NiO, respectively.

Under air, $Pr_4Ni_3O_{10+\delta}$ is thermally stable up to about 1050°C. Above this temperature decomposition starts to occur and a complete decomposition into $Pr_2NiO_{4+\delta}$ and NiO is achieved at around 1150 °C. The decomposition is completely irreversible under air, as the decomposition product, $Pr_2NiO_{4+\delta}$, is instable under these conditions. Under argon the same behaviour is observed, however the decomposition temperature is lower than under air (900°C instead of 1050°C), and the weight loss after the decomposition is larger than in air, probably because of the larger evolution (decrease) of the oxygen over-stoichiometry of $Pr_2NiO_{4+\delta}$ under argon. Under oxygen, $Pr_4Ni_3O_{10+\delta}$ shows higher stability than in air, up to 1120 °C. Again above this temperature it decomposes into $Pr_2NiO_{4+\delta}$ and NiO. Upon cooling, however, a weight uptake is observed around 950 °C, which is the signature of the formation of the more oxidized phase $Pr_4Ni_3O_{10+\delta}$ along with PrO_x, as attested by the presence of these phase in the decomposition mixture upon cooling (Table 2). This result is in good agreement with what was observed on pure $Pr_2NiO_{4+\delta}$ upon cooling under oxygen [21, 32]

Regarding $La_4Ni_3O_{10+\delta}$, we chosen to perform TGAs up to 1200°C *only*, *i.e.* at the maximum temperature for which the thermal stability of the material is ensured under air according to the literature [33].

This hypothesis was not confirmed here since the XRD performed after TGA under air showed a light chemical decomposition of the material around 1150°C- 1190°C (Table 2). The decomposition products are NiO and $La_3Ni_2O_{7\pm\delta}$. The experiment under air - showed a very small mass loss below around 1050°C, which then accelerates sharply. This indicates a partial thermal reduction resulting from a loss of oxygen over-stoichiometry. Interestingly, this loss of oxygen is completely reversible. Finally, under O_2 a very light degradation takes place forming $La_2NiO_{4+\delta}$ and NiO.

The thermal behaviour of $La_3PrNi_3O_{10+\delta}$ differs from that of $La_4Ni_3O_{10+\delta}$. Under air the acceleration of the mass loss beyond around 1050°C is much greater for $La_3PrNi_3O_{10+\delta}$. In addition, the cooling behaviour of the material is non-reversible and a thermal decomposition is observed. The thermal stability domain of $La_3PrNi_3O_{10+\delta}$ is therefore lower than that of $La_4Ni_3O_{10+\delta}$ under air, and the decomposition products are to those from the experiments conducted on $Pr_4Ni_3O_{10+\delta}$ [21, 32], plus some $La_{2-x}Pr_xNiO_{4+\delta}$ (n=1 phase). Under O_2, $La_3PrNi_3O_{10\pm\delta}$ slightly degrades into the n=2 and 1 members as well as nickel oxide above 1190 °C, while the n=3 phase seems to be completely re-formed upon cooling.

Finally, under argon the behaviour of the two oxides is very similar to the one of $Pr_4Ni_3O_{10+\delta}$: as expected the thermal stability is limited to 940 and 990°C for $La_4Ni_3O_{10+\delta}$ and $La_3PrNi_3O_{10+\delta}$, respectively; like for $Pr_4Ni_3O_{10+\delta}$, the n=2 terms ($La_2NiO_{4+\delta}$ and (La, Pr)$_2NiO_{4+\delta}$, respectively), plus NiO, are formed upon cooling.

Table 2 - Stability limit and degradation products in air, argon and O_2

Material	Stability limit – O_2	Degradation products in O_2 after the cooling cycle	Stability limit - air	Degradation products in air after the cooling cycle	Stability limit - Ar	Degradation products in Ar after the cooling cycle
$La_4Ni_3O_{10\pm\delta}$	>1190°C	None	1150 °C	$La_3Ni_2O_{7\pm\delta}$, NiO	940 °C	$La_2NiO_{4+\delta}$ + NiO
$La_3PrNi_3O_{10\pm\delta}$	>1190°C	$La_{3-x}Pr_xNi_2O_{7\pm\delta}$, $La_{4-x}Pr_xNi_3O_{10\pm\delta}$, $La_{2-x}Pr_xNiO4_{+\delta}$	1150°C	$La_{3-x}Pr_xNi_2O_{7\pm\delta}$, $La_{2-x}Pr_xNiO_{4+\delta}$, $La_{1-x}Pr_xNiO_{3-\delta}$, NiO	990 °C	$La_{2-x}Pr_xNiO4_{+\delta}$ + NiO
$Pr_4Ni_3O_{10\pm\delta}$ [21]	1120°C	$Pr_4Ni_3O_{10\pm\delta}$, $Pr_2NiO_{4+\delta}$, NiO, PrO_x	1050°C	$Pr_2NiO_{4+\delta}$	900 °C	$Pr_2NiO_{4+\delta}$ + NiO

3.3.2. Long term oxide thermal stability at the SOC working temperature

Investigation of the thermal stability of the three materials was performed at 600°C, 700°C, and 800°C for one month, and three months. Results of the XRD analysis are shown in Fig. S.I. 6 (one month duration) and Fig. 7 (three months duration), respectively. All three oxides are stable at the operating temperatures for a large duration. The great stabilities of $Pr_4Ni_3O_{10+\delta}$

and $La_4Ni_3O_{10+\delta}$ are confirmed and $La_3PrNi_3O_{10+\delta}$ is found to have the same promising stability.

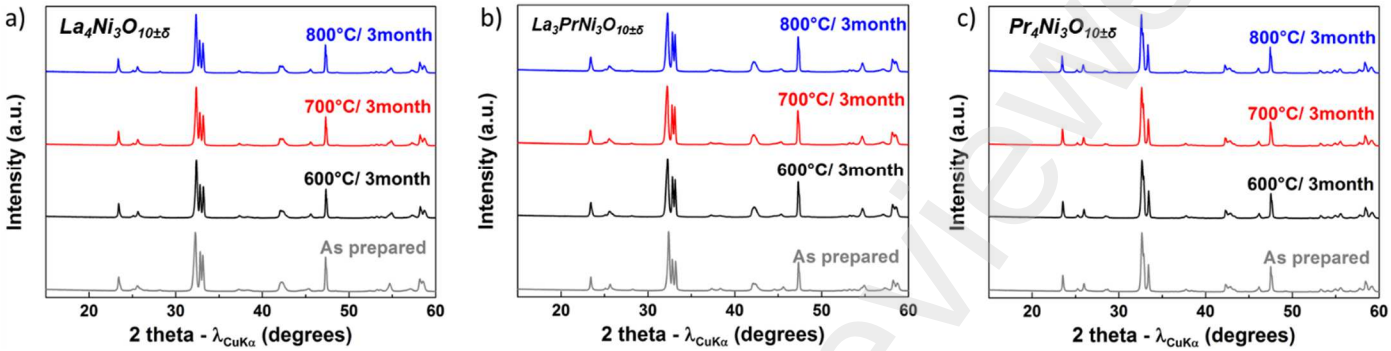

Fig. 7. Diffractograms of the as-synthesized phase and, after 3 months at 600°C, 700°C and 800°C for (a) $La_4Ni_3O_{10+\delta}$, (b) $La_3PrNi_3O_{10+\delta}$ and (c) $Pr_4Ni_3O_{10+\delta}$

Moreover, the thermal variation of the oxygen content was also investigated over the stability domain of $Pr_4Ni_3O_{10+\delta}$ under argon, *i.e.* from room temperature to 800 °C. Before starting the experiment, the powder was first equilibrated under air, ensuring the starting value of $\delta \sim 0.10$. The thermal variation of the oxygen content, $10+\delta$, is plotted in Fig. 8. During the first cycle, an irreversible weight loss is observed while in the second one an almost reversible behaviour is noticed.

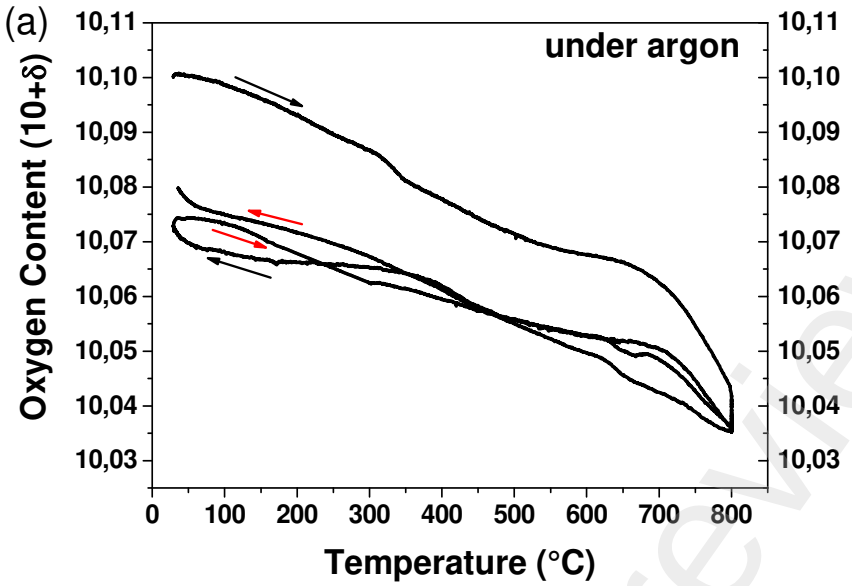

Fig.8 - Thermal variation of the oxygen content (10+δ) for $Pr_4Ni_3O_{10+\delta}$ under argon (30 °C ≤ T ≤ 800 °C)

As a concluding point, this work focusing on the thermal stability of Pr-Ni based nickelates belonging to the RP series, namely: $Pr_4Ni_3O_{10+\delta}$, $La_4Ni_3O_{10+\delta}$, $La_3PrNi_3O_{10+\delta}$ (n=3), and $PrNiO_{3-\delta}$ (n = ∞), gives useful trends in particular to synthesize and sinter the considered oxides.

4. Conclusion

We have studied the thermal stability of four Pr-Ni based oxide materials belonging to the RP series: $Pr_4Ni_3O_{10+\delta}$, $La_4Ni_3O_{10+\delta}$, $La_3PrNi_3O_{10+\delta}$ (n=3), and $PrNiO_{3-\delta}$ (n = ∞), under three atmospheres: oxygen, air, and argon. We focused on Pr as main rare-earth of the considered compositions because of the interesting electrochemical properties of several compositions.

The conclusions would be used as useful guidelines for the sintering of the electrodes prior to their electrochemical characterizations.

$PrNiO_{3-\delta}$ phase is stable only up to 800, 1000 and 1100 °C under argon, air and oxygen, respectively. $Pr_4Ni_3O_{10+\delta}$ phase is stable only up to 900, 1050 and 1100 °C under argon, air and oxygen, respectively. It dissociates completely into $Pr_2NiO_{4+\delta}$ and NiO above the specified temperature. $La_4Ni_3O_{10+\delta}$ show partial decomposition into NiO and $La_3Ni_2O_{7\pm\delta}$ at ~1150 °C. The thermal stability of $La_3PrNi_3O_{10+\delta}$ is even lower than that of $La_4Ni_3O_{10+\delta}$ under air, and the main decomposition products are identical to those from the experiments carried out with $Pr_4Ni_3O_{10+\delta}$. However, both materials are completely stable in an oxygen atmosphere up to 1200 °C.

We are aware that these observations are largely governed by kinetics and a more comprehensive study would require taking into account the thermodynamics of the system, which is however not available to the best of our knowledge. Regardless of the material considered, the upper available temperature appears too low for the sintering under metal supported cells (MSCs) conditions, especially for $PrNiO_{3-\delta}$. In this last case, the upper available temperature limit under air and O_2 is probably a parameter that explains the rather low electrochemical properties of the material. A way to explore would be to develop composites with GDC as electrodes to be sintered on 8YSZ. Regarding the Pr-Ni based materials belonging to the term n=3 of the series, like for the corresponding term n=1, the stability is improved when limiting the Pr amount, again substituting 25% of La with Pr seems to be a good compromise. The electrochemical measurements are in progress.

Acknowledgements

This work benefited from state support managed by the Agence Nationale de la Recherche under the France 2030 program, referenced ANR-22-PEHY-0008 (project CELCER – PEPR

H2 decarbonized). The authors also acknowledge Eric Lebraud (ICMCB) for XRD, Cathy Denage (ICMCB) and Marina Soustre (IRCER, Limoges) for thermal measurements.

References

[1] S.H. Jensen, C. Graves, M. Mogensen, C. Wendel, R. Braun, G. Hughes, Z. Gao, S.A. Barnett, Large-scale electricity storage utilizing reversible solid oxide cells combined with underground storage of CO2 and CH4, Energy & Environmental Science, 8 (2015) 2471-2479.
[2] M.A. Morales-Zapata, A. Larrea, M.A. Laguna-Bercero, Lanthanide nickelates for their application on Solid Oxide Cells, Electrochimica Acta, 444 (2023) 141970.
[3] A.P. Tarutin, J.G. Lyagaeva, D.A. Medvedev, L. Bi, A.A. Yaremchenko, Recent advances in layered Ln2NiO4+δ nickelates: fundamentals and prospects of their applications in protonic ceramic fuel and electrolysis cells, Journal of Materials Chemistry A, 9 (2021) 154-195.
[4] G. Amow, S.J. Skinner, Recent developments in Ruddlesden–Popper nickelate systems for solid oxide fuel cell cathodes, Journal of Solid State Electrochemistry, 10 (2006) 538-546.
[5] V. Vibhu, A.R. Hanifi, T.H. Etsell, J.-M. Bassat, Oxygen Electrode Materials for Solid Oxide Electrolysis Cells (SOECs), in: M.A. Laguna-Bercero (Ed.) High Temperature Electrolysis, Springer International Publishing, Cham, 2023, pp. 59-89.
[6] A. Egger, N. Schrödl, C. Gspan, W. Sitte, La2NiO4+δ as electrode material for solid oxide fuel cells and electrolyzer cells, Solid State Ionics, 299 (2017) 18-25.
[7] C. Ferchaud, J.-C. Grenier, Y. Zhang-Steenwinkel, M.M.A. van Tuel, F.P.F. van Berkel, J.-M. Bassat, High performance praseodymium nickelate oxide cathode for low temperature solid oxide fuel cell, Journal of Power Sources, 196 (2011) 1872-1879.
[8] A. Flura, S. Dru, C. Nicollet, V. Vibhu, S. Fourcade, E. Lebraud, A. Rougier, J.-M. Bassat, J.-C. Grenier, Chemical and structural changes in Ln2NiO4+δ (Ln=La, Pr or Nd) lanthanide nickelates as a function of oxygen partial pressure at high temperature, Journal of Solid State Chemistry, 228 (2015) 189-198.
[9] S.J. Kim, K.J. Kim, A.M. Dayaghi, G.M. Choi, Polarization and stability of La2NiO4+δ in comparison with La0.6Sr0.4Co0.2Fe0.8O3−δ as air electrode of solid oxide electrolysis cell, International Journal of Hydrogen Energy, 41 (2016) 14498-14506.
[10] A.D. Rougier, A. Flura, C. Nicollet, V. Vibhu, S. Fourcade, E. Lebraud, J.-M. Bassat, J.-C. Grenier, Ln2NiO4+δ (Ln = La, Pr) As Suitable Cathodes for Metal Supported Cells, ECS Transactions, 68 (2015) 817-823.
[11] S. Saher, J. Song, V. Vibhu, C. Nicollet, A. Flura, J.-M. Bassat, H.J.M. Bouwmeester, Influence of annealing at intermediate temperature on oxygen transport kinetics of Pr2NiO4+δ, Journal of Materials Chemistry A, 6 (2018) 8331-8339.
[12] E. Boehm, J.M. Bassat, P. Dordor, F. Mauvy, J.C. Grenier, P. Stevens, Oxygen diffusion and transport properties in non-stoichiometric Ln2−xNiO4+δ oxides, Solid State Ionics, 176 (2005) 2717-2725.
[13] E. Boehm, J.M. Bassat, M.C. Steil, P. Dordor, F. Mauvy, J.C. Grenier, Oxygen transport properties of La2Ni1−xCuxO4+δ mixed conducting oxides, Solid State Sciences, 5 (2003) 973-981.
[14] G. Amow, P.S. Whitfield, I.J. Davidson, R.P. Hammond, C.N. Munnings, S.J. Skinner, Structural and sintering characteristics of the La2Ni1−xCoxO4+δ series, Ceramics International, 30 (2004) 1635-1639.
[15] S. Nishimoto, S. Takahashi, Y. Kameshima, M. Matsuda, M. Miyake, Properties of La2-xPrxNiO4 cathode for intermediate-temperature solid oxide fuel cells, Journal of the Ceramic Society of Japan, 119 (2011) 246-250.
[16] V. Vibhu, A. Rougier, C. Nicollet, A. Flura, J.-C. Grenier, J.-M. Bassat, La2−xPrxNiO4+δ as suitable cathodes for metal supported SOFCs, Solid State Ionics, 278 (2015) 32-37.

[17] V. Vibhu, A. Flura, A. Rougier, C. Nicollet, S. Fourcade, T. Hungria, J.-C. Grenier, J.-M. Bassat, Electrochemical ageing study of mixed lanthanum/praseodymium nickelates La2-xPrxNiO4+δ as oxygen electrodes for solid oxide fuel or electrolysis cells, Journal of Energy Chemistry, 46 (2020) 62-70.
[18] A.V. Kovalevsky, V.V. Kharton, A.A. Yaremchenko, Y.V. Pivak, E.N. Naumovich, J.R. Frade, Stability and oxygen transport properties of Pr2NiO4+δ ceramics, Journal of the European Ceramic Society, 27 (2007) 4269-4272.
[19] M.A. Laguna-Bercero, H. Monzón, A. Larrea, V.M. Orera, Improved stability of reversible solid oxide cells with a nickelate-based oxygen electrode, Journal of Materials Chemistry A, 4 (2016) 1446-1453.
[20] C. Nicollet, A. Flura, V. Vibhu, A. Rougier, J.-M. Bassat, J.-C. Grenier, An innovative efficient oxygen electrode for SOFC- Pr6O11 infiltrated into Gd-doped ceria backbone, International Journal of Hydrogen Energy.
[21] V. Vibhu, A. Rougier, C. Nicollet, A. Flura, S. Fourcade, N. Penin, J.-C. Grenier, J.-M. Bassat, Pr4Ni3O10+δ: A new promising oxygen electrode material for solid oxide fuel cells, Journal of Power Sources, 317 (2016) 184-193.
[22] J.-M. Bassat, V. Vibhu, C. Nicollet, A. Flura, S. Fourcade, J.-C. Grenier, A. Rougier, Comparison of Pr-Based Cathodes for IT-SOFCs in the Ruddlesden-Popper Family, ECS Transactions, 78 (2017) 655-665.
[23] V. Vibhu, Stability and ageing studies of praseodymium-based nickelates as cathodes for Solid Oxide Fuel Cells, PhD Thesis, Université de Bordeaux, 2016.
[24] V. Vibhu, A. Flura, C. Nicollet, S. Fourcade, N. Penin, J.-M. Bassat, J.-C. Grenier, A. Rougier, M. Pouchard, Characterization of PrNiO3-δ as oxygen electrode for SOFCs, Solid State Sciences, 81 (2018) 26-31.
[25] P. Courty, H. Ajot, C. Marcilly, B. Delmon, Oxydes mixtes ou en solution solide sous forme très divisée obtenus par décomposition thermique de précurseurs amorphes, Powder Technology, 7 (1973) 21-38.
[26] R. Frugier, V. Vibhu, S. Fourcade, J.M. Bassat, J. Gamon, Mixed La/Pr n=3 Ruddkesden-Popper nickelates as stable and efficient oxygen electrodes for high temperature water electrolysis, Proceeding of the 16th European SOFC and SOE Forum, Luzern (CH) (2024).
[27] J. Rodríguez-Carvajal, Recent advances in magnetic structure determination by neutron powder diffraction, Physica B: Condensed Matter, 192 (1993) 55-69.
[28] C.D. Ling, D.N. Argyriou, G. Wu, J.J. Neumeier, Neutron Diffraction Study of La3Ni2O7: Structural Relationships Among n=1, 2, and 3 Phases Lan+1NinO3n+1, Journal of Solid State Chemistry, 152 (2000) 517-525.
[29] M.A. Yatoo, I.D. Seymour, S.J. Skinner, Neutron diffraction and DFT studies of oxygen defect and transport in higher-order Ruddlesden–Popper phase materials, RSC Advances, 13 (2023) 13786-13797.
[30] C.-Y. Tsai, A. Aguadero, S.J. Skinner, High electrical conductivity and crystal structure of the solid oxide cell electrode Pr4Ni3O10-δ, Journal of Solid State Chemistry, 289 (2020) 121533.
[31] M.J. Martinez-Lope, J.A. Alonso, Thermal stability of rare-earth nickelates Part I: the RNiO3 (R=La,Pr,Nd,Sm,Eu) perovskites, European Journal of Solid State and Inorganic Chemistry, 32 (1995) 361-371.
[32] P. Odier, C. Allançon, J.M. Bassat, Oxygen Exchange in Pr2NiO4+δ at High Temperature and Direct Formation of Pr4Ni3O10−x, Journal of Solid State Chemistry, 153 (2000) 381-385.
[33] M. Zinkevich, N. Solak, H. Nitsche, M. Ahrens, F. Aldinger, Stability and thermodynamic functions of lanthanum nickelates, Journal of Alloys and Compounds, 438 (2007) 92-99.

Supplementary informations

Fig. S.I. 1.: XRD diagrams of the as-prepared materials

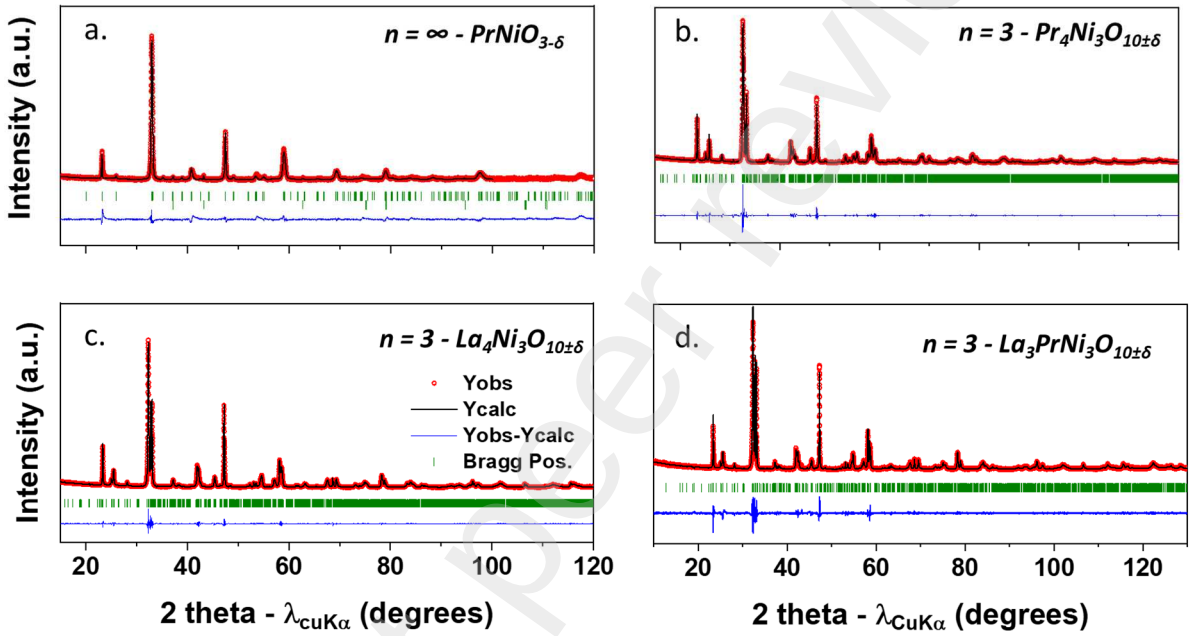

Fig. S.I. 2.: XRD analysis performed on $PrNiO_{3-\delta}$ after quenching from 1050°C under air and 1070°C under oxygen

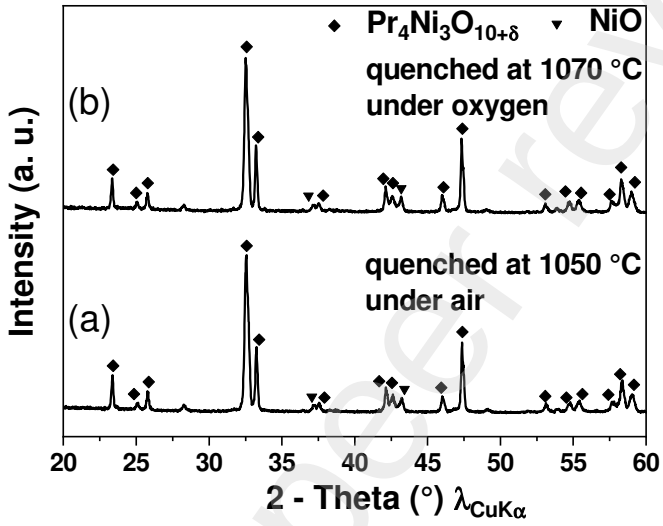

Fig. S.I. 3.: Additional TGAs performed on $PrNiO_{3-\delta}$ under oxygen

While heating under oxygen $PrNiO_{3-\delta}$ is fully dissociated into $Pr_2NiO_{4+\delta}$ and NiO above 1120 °C, the cooling behavior is different. The TGA plots of $PrNiO_{3-\delta}$ performed under oxygen successively at 2°, then 5° and finally 1° C.min^{-1} are reported in **Figures SI 3a, b** and **c** respectively.

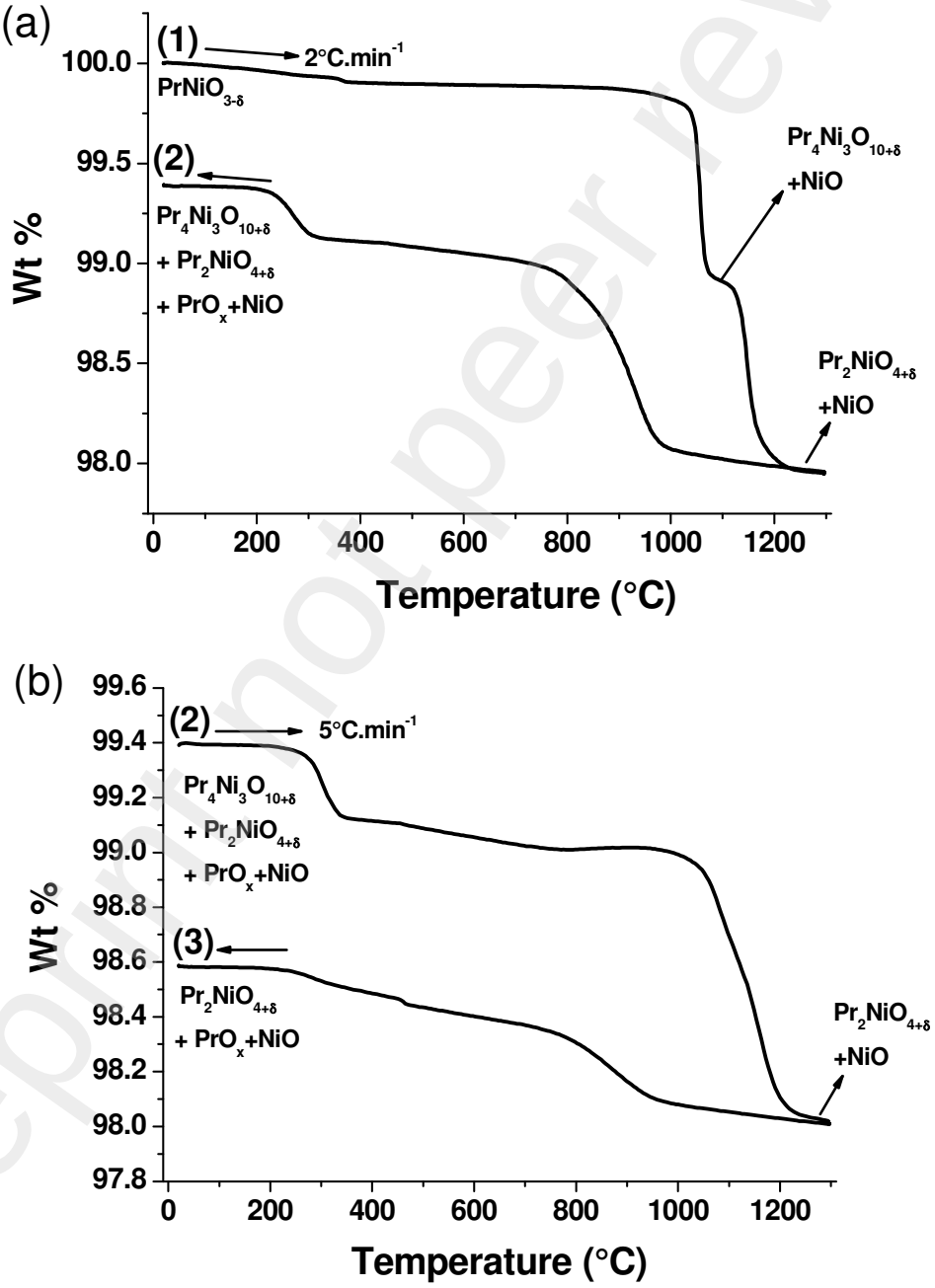

(c)

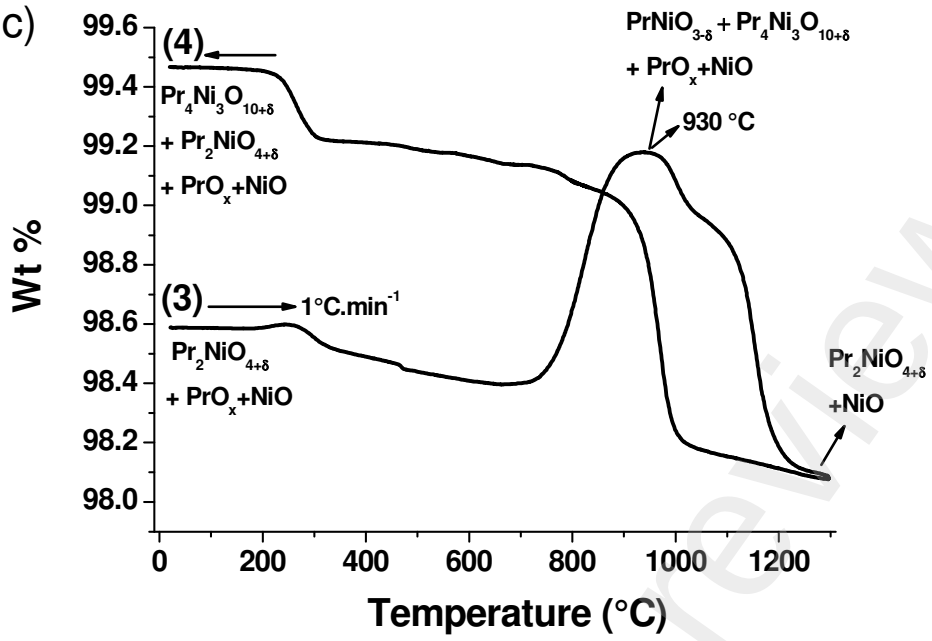

Fig. S.I. 4.: Thermal stability of $PrNiO_{3-\delta}$, with the derivatives formed under air, oxygen and argon during (a) heating and (b) cooling, as a function of the heating and cooling rates

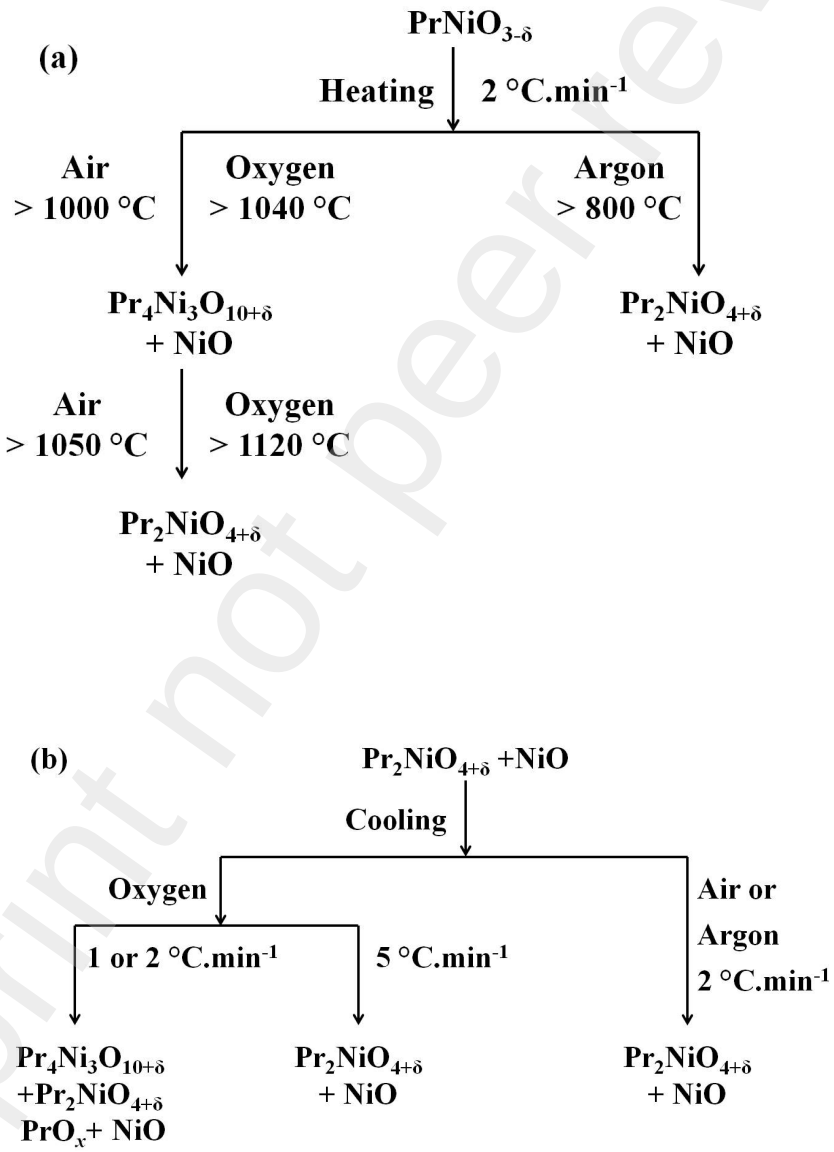

Fig. S.I. 5: X-ray diffractograms of $PrNiO_{3-\delta}$ powder, after TGA experiment under oxygen (30 °C ≤ T ≤ 1000 °C) with the rate of 2 °C.min^{-1} for different dwell times of 2 h and 3 h at 1000 °C

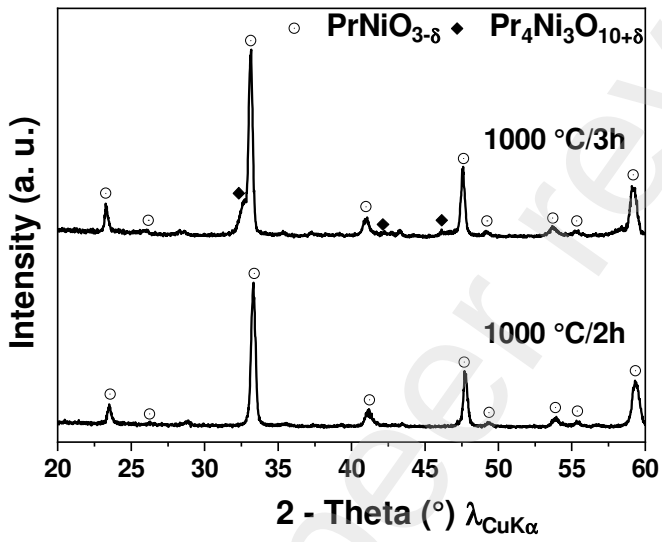

Fig. S I 6: Diffractograms of the as-synthesized phase, and after one month at 600°C, 700°C and 800 °C for (a) $La_4Ni_3O_{10+\delta}$, (b) $La_3PrNi_3O_{10+\delta}$ and (c) $Pr_4Ni_3O_{10+\delta}$